



Fluid Flow Analysis of Porous Metals in Solar Thermal Applications

Radim Rybár^{a*}, Michal Kalavský^b

^{a,b}*Technical University of Košice, Faculty of Mining, Ecology, Process Control and Geotechnology, Institute of Earth Resources, Letná 9, 042 00 Košice, Slovak Republic*

^a*Email: radim.rybar@tuke.sk*

^b*Email: michal.kalavsky.2@tuke.sk*

Abstract

Presented paper dealt with use of porous materials, in this case metal foam, in the solar thermal applications. First part of paper is engaged to the fluid flow analysis in the spatial structure of metal foam body, which represents simplified form of the solar absorber. From application point of view were desired properties of foam structure described with using of CFD tools based on finite element method. As a boundary conditions of simulation were set different heat transfer flow rates and properties of metal foam which is characterized by average pore diameter. According to obtained results of simulations were identified optimal conditions and flow regimes for metal foam that will be used as a full flow solar flat collector.

Keywords: metal foam; flow analysis; finite element method; solar flat collector.

* Corresponding author.

1. Introduction

Materials with cellular structure nature use in the construction of largest and strongest natural objects, whether there are bones, wood or corals, cellular structure provides unique properties of this material. Industrial use of materials with cellular structure has been recently very limited with level of technological development, as to the latest knowledge and advanced manufacturing technology allowed "copying" the nature and deployment of these materials in various industries and applications[1,2]. One of the groups of materials with cellular structure represents metal foams (hereinafter MF) [3]. These are materials with a large number of cells in the base material - metal. These cells can form an interconnected solid pillars or plates, which form the edges and cell walls [4]. Cells of MF may be closed, in this case it is a MF with a closed structure, or may create a connected network extending across the whole volume of material, in this case it is an open structured MF [5].

Unique internal structure of porous materials makes them suitable for use in heat transfer, filtration of liquids and gases, acoustics and refractory. Using of MF records in solar technology in recent years a growing trend. Recently been published several technical solutions for the flat absorbers, heat exchangers, foam insulation for use in solar technology. In the paper [6] is published application of MF in the role of the absorber plates, which aims to increase the effective cross-section blades, while maintaining low weight, which is an alternative solution to conventional blade (Figure 1a). Here applies the heat transfer by conduction. In terms of features of the heat exchanger, where it is already heat transfer by convection, it is considered using the MF in the design of coaxial countercurrent heat exchanger described [7], where MF fills the annular space, thus significantly increasing the heat exchange surface (Figure 1b).

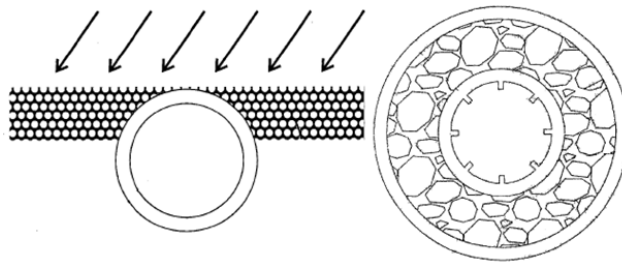


Figure 1: An example of use of MF, absorber of full flow solar collector (a) and as a annular heat exchanger (b)

Researched and published technical solutions and relevant publications pointed out, that these cover a range of possibilities for using of MF in solar technology only partially, creating space for the application of other innovative solutions, the basic conceptual features have been developed already during the development in [8,9,10,11]partially published concept of a solar collector, respectively, during the execution of experiments aimed at detecting performance characteristics of vacuum tube collectors and construction of experimental solar system.

Contrary to some published solutions, we focused on the development of solar absorbers based on full flow plate forms with an open pore structure, with the possibility of a parallel arrangement of channels. In terms of utilization in solar thermal technology is therefore important to examine the properties of MF with an open

structure, particularly in relation to the performance features of solar energy capture, mediation photo thermal conversion, heat transfer through body from MF, heat transfer to medium, aspects of the media flow through structure from MF, the definition of hydraulic flow channels, etc. For optimal use of MF properties and required functions, our attention was primarily focused on convection heat transfer fluid in the inner structure of MF. One of the tools, which can help achieve better idea of the actions and their detailed analytical solution, are CAD tools for analyzing the flow of media, using the finite element calculation method.

Based on data published in [12], is study of the internal structure of the MF by using CAD systems are currently focused primarily on describing mathematically the exact geometric shapes forming the cell structure and transformation of these mathematical structures in the CAD environment. In Adhaziev and his colleagues [12] states that before the study focused mainly on describing the density of foam metals using basic mathematical tools Boolean operations.

Schroeder and his colleagues [13] suggests the use of stochastic functions as a means of representation of porosity, which can be seen as complementary data on the density of porous materials. This allows to specify not only the material and the pore volume, but also describe the properties of the pore (size and roughness). On that basis, according to research results published in [13], appears the need for extending the Boolean operations in the area of porous solids, where objects are characterized by different geometry, density, porosity, etc. this is a design system for creating CSG (Constructive Solid Geometry) model of heterogeneous objects, with which it would be possible to perform the analysis necessary for the production and design practice. CSG is based on mathematically difficult apparatus, which effective use expected efficient computing.

Because our work is focused mainly on structural aspects of the designed solar absorber our analysis and models were performed in an environment of CAD software working on the principle of finite elements methods, which conveniently connects the user-friendly environment in the design phase and sufficiently representative results of simulations and analysis. It is used to simulate stress, strain, heat flow, fluid flow etc. Simulations runs on defined model. The principle of the finite element method is discretization of the continuous continuum into finite elements, while the detected parameters are determined by the individual nodal point.

2. Flow characteristics of MF

The concept of permeability of porous materials was published by Darcy in 1856 in [14]. Based on laboratory experiments with flow of water through sand filled volume Darcy disagreed empirical equation for estimating volume flow:

$$Q = k.A \frac{dp}{dx} \quad (1)$$

where k is the coefficient of filtration depending on the type of porous material, x is the length of flow path, dp is the difference in hydrostatic pressure when passing the test sample and A is the cross sectional area of the specimen. This equation is limited in many aspects, such as its use is appropriate only for incompressible

Newtonian fluid and slow isometric flow through the relatively long, uniform and isotropic porous body with a low coefficient of filtration. Therefore, Darcy's law in many states in the form of literature:

$$\frac{dp}{dx} = \frac{\mu}{K}V \quad (2)$$

where k is replaced by (μ / K) , where K is the specific permeability, which is independent of the properties of flowing liquids and μ is the dynamic viscosity of a liquid [15]. This equation is known as the Hazen-Darcy equation, which applies to the pressure drop unit length of flow through porous media as a relationship between flow velocity and dynamic viscosity. The next stage in the development of a mathematical description of flow through porous media environment is the Hazen-Dupit-Darcy equation, which considerate the size of resistive forces, depending on the square velocities:

$$\frac{dp}{dx} = \frac{\mu}{K}V + \rho cV^2 \quad (3)$$

where dx represents the thickness, respectively length of porous media (depending on the direction of flow), dp is the pressure drop over a length dx , V is the velocity of the medium, ρ is the density of the flowing medium, μ is the viscosity of the flowing medium, K is the permeability of the porous medium and C is the drag coefficient of porous media [16]. In this equation ρcV^2 expresses the effect of inertia. Davis and his colleagues in [17] showed that experimental data are presented for high values of Darcy velocity are preferable to the quadratic equation form. If the velocity increases, the effects of inertia and turbulence become significant elements of flow and pressure gradient values have a parabolic shape of the graphic display. At high velocities, the flow is characterized as non-Darcy flow (depending on the Reynolds number). This flow has a linear character and pressure loss reaches higher values than the Darcy type of flow [18].

Due to the complex internal structure of the MF is more accurate experimental determination of permeability of different types of MF than mathematical modeling of MF. Until now, few published experimental studies, in part correlated with the actual permeability of the MF. Boomsma and his colleagues showed that the values of velocity 0.110 m.s^{-1} leads to changes in flow regime from Darcy to non-Darcy flow [18]. Diedericks and Du Plesiss in [19] demonstrated that the coefficient C (drag coefficient of porous media) is just as important and decisive as velocity increase. Then the resistive force becomes the dominant factor and must be taken into consideration in the analysis of the pressure loss of these materials (depending on porosity).

Bhattacharya and his colleagues in [3] presented a comprehensive analytical and experimental research to determine the effective thermal conductivity and permeability of the MF. According to the results of the permeability increases with the pore diameter and porosity of the MF and the inertia coefficient is associated only with the total porosity of MF. Recently published results Khayargoli and his colleagues [16] revealed that with increasing pore diameter increases the permeability and inertia coefficient has a decreasing trend. Interesting finding is that the examination of MF with a porosity of 83 and 90% have found that with decreasing pore diameter increases the specific surface, resulting in increased resistance to fluid flow forces.

From the above facts that the area of study for the MF in terms of the flow medium is still widely unexplored area with very different results of experiments. This on the one hand offers the possibility of scientific research in areas relatively attractive, but on the other hand, greatly hampers the implementation of accurate analysis and design for the industry, since it is not possible to precisely define the characteristics of MF.

3. Methodology

Realized development is directed to the design of the solar collector, which served as the absorber - photothermal converter - heat exchanger. The design considers the entire flow cross-section of the body, which will be hydraulically defined flow into channels. Provisionally considered with direct insolation of object, which is not further specified. In the first stage of solving the problem it was necessary to implement a series of simulations aimed at the description of the hydraulic processes and their quantification. For the design of element analysis has been studied in a simplified form of the full flow plates $500 \times 100 \times 10$ mm. Description of processes using mathematical modeling will form the basis for the second phase of the investigation - and subsequent experimental verification of the specification of shape and size parameters. Analytical tool, which analyzes were performed each working with a mathematical tool Navier-Stokes equations (4), which define the mass, momentum and energy conservation law for fluid flow.

$$\frac{\partial u_i}{\partial t} + (u, \nabla)u_i = -\rho^{-1} \frac{\partial p}{\partial x_i} + \nu \Delta u_i + f_i \quad (4)$$

where u is velocity, ρ - fluid density, p - pressure of the fluid, ν - kinematic viscosity, f - the sum of the volume forces.

These equations are supplemented by the equations characterizing the fluid, and the empirical dependence of density of liquids, viscosity and thermal conductivity of the fluid temperature. The analysis is ultimately specified by its geometry, boundary and initial conditions. The used CAD tool is based on defined specifications able to identify the laminar and turbulent flow. The laminar flow occurs at low Reynolds number, which is defined as the sum of the representative values for the speeds and lengths divided by the kinematic viscosity of liquids. If the value of the Reynolds number exceeds a certain threshold, the flow becomes turbulent, i.e. that the various flow parameters are randomly changed.

The above-mentioned identification of turbulent flow occurs using Favre-Navier-Stokes equations, where the average time for the effect of turbulence in fluid flow calculation only partially taken into account, while other time-dependent phenomena are reflected directly and immediately. Through this process, other variables such as Reynolds number is in the process of calculation to be included in the equations requiring additional information entered by the user. For more advanced calculations using equations dealing with the kinetic energy and its dissipation rate, for this purpose, the use of $k-\varepsilon$ model. CAD software uses a single system of equations to describe the laminar and turbulent flow, makes it possible for the calculation of transition from laminar to turbulent flow and back. The definitions of the law of conservation of mass, momentum and energy, expressed in Cartesian coordinate system is used the following definition:

$$\frac{\partial \rho}{\partial t} + \frac{\partial}{\partial x_i}(\rho u_i) = 0 \quad (5)$$

$$\frac{\partial \rho}{\partial t} + \frac{\partial}{\partial x_j}(\rho u_i u_j) + \frac{\partial p}{\partial x_i} = \frac{\partial}{\partial x_j}(\tau_{ij} + \tau_{ij}^R) + S_i, i = 1, 2, 3 \quad (6)$$

$$\frac{\partial \rho H}{\partial t} + \frac{\partial \rho u_i H}{\partial x_i} = \frac{\partial}{\partial x_i} \left(u_j (\tau_{ij} + \tau_{ij}^R) + q_i \right) + \frac{\partial p}{\partial t} - \tau_{ij}^R \frac{\partial u_i}{\partial x_j} + \rho \varepsilon + S_i u_i + Q_H \quad (7)$$

$$H = h + \frac{u^2}{2} \quad (8)$$

where u is velocity, ρ is the density of liquid S_i is the force per unit mass defined by the size of the resistive forces of porous media $S_{iporous}$; buoyancy forces $S_{igravity} = -\rho g_i$ where g_i is the gravitational acceleration in the i -direction of grid system, and forces caused rotation of the S_i rotation, therefore we can write $S_i = S_{iporous} + S_{igravity} + S_{rotation}$, h is enthalpy, Q_H is the heat flow value, τ_{ik} is the viscous shear stress tensor, q_i is flow of heat diffusion. To calculate the fluid flow Mach number is used the following relationship:

$$\frac{\partial \rho E}{\partial t} + \frac{\partial \rho u_i \left(E + \frac{p}{\rho} \right)}{\partial x_i} = \frac{\partial}{\partial x_i} \left(u_j (\tau_{ij} + \tau_{ij}^R) + q_i \right) - \tau_{ij}^R \frac{\partial u_i}{\partial x_j} + \rho \varepsilon + S_i u_i + Q_H \quad (9)$$

$$E = e + \frac{u^2}{2}, \quad (10)$$

where e is the internal energy. For Newtonian fluid is viscous stress tensor shear defined:

$$\tau_{ij} = \mu \left(\frac{\partial u_i}{\partial x_j} + \frac{\partial u_j}{\partial x_i} - \frac{2}{3} \delta_{ij} \frac{\partial u_k}{\partial x_k} \right), \quad (11)$$

For the definition of kinetic energy and turbulent energy dissipation and laminar flow CAD software uses equations:

$$\frac{\partial \rho k}{\partial t} + \frac{\partial}{\partial x_i}(\rho u_i k) = \frac{\partial}{\partial x_i} \left(\left(\mu + \frac{\mu_t}{\sigma_k} \right) \frac{\partial k}{\partial x_i} \right) + S_k, \quad (12)$$

$$\frac{\partial \rho \varepsilon}{\partial t} + \frac{\partial}{\partial x_i}(\rho u_i \varepsilon) = \frac{\partial}{\partial x_i} \left(\left(\mu + \frac{\mu_t}{\sigma_\varepsilon} \right) \frac{\partial \varepsilon}{\partial x_i} \right) + S_\varepsilon, \quad (13)$$

where S_k and S_a are defined as:

$$S_k = \tau_{ij}^R \frac{\partial u_i}{\partial x_j} - \rho \varepsilon + \mu_t P_B, \quad (14)$$

$$S_\varepsilon = C_{\varepsilon 1} \frac{\varepsilon}{k} \left(f_1 \tau_{ij}^R \frac{\partial u_i}{\partial x_j} + \mu_t C_B P_B \right) - C_{\varepsilon 2} f_2 \frac{\rho \varepsilon^2}{k}, \quad (15)$$

Here P_B represents the turbulent component derived from buoyant forces:

$$P_B = -\frac{g_i}{\sigma_B} \frac{1}{\rho} \frac{\partial \rho}{\partial x_i}, \quad (16)$$

where g_i is the gravitational acceleration component in the direction x_i and f_1 and f_2 represent turbulence factor and are a function of Re (Reynolds number, respectively Reynolds stress tensor) [20].

Analyses were performed for different types of porosity and for different values of volume flow heat transfer medium as shown in Tab. 1 and Tab. 2.

As streaming media was used water ($\rho = 998 \text{ kg m}^{-3}$, $t = 55 \text{ }^\circ\text{C}$).

Table 1: Porosity used in fluid flow analysis

Pore diameter [μm]	220	330	550	1000	1600
PPI	159	75	45	25	15
Porosity [%]	75	80	85	90	93
Density [$\text{g}\cdot\text{cm}^{-3}$]	2.3	1.8	1.0	0.9	0.6

Table 2: An overview of the flow parameters used in the analysis

Flow through collector [$\text{l}\cdot\text{h}^{-1}$]	10	50	100	150
Flow in segment [$\text{l}\cdot\text{h}^{-1}$]	0,5	2,5	5	7,5
Flow in segment [$\text{m}^3\cdot\text{s}^{-1}$]	1.385E-07	6.9E-07	1.385E-06	2.08E-06

Flow analysis was performed with MF whose properties have been defined as a function of pore size and type of flow cell was defined as multidirectional flow with possible turbulence element (due to higher flow rates and higher values of velocity) by Boomsma and his colleagues [18].

4. Results and discussion

Different MF structures analyses results showed a vision about pressure loss caused by heat transfer medium flow. Also vision about transfer medium flow speed was gained. Figure 2 and 3 show an example of pressure maps, respectively view of trajectories and flow speed obtained by the simulations. The pressure reduction from input to output in whole MF cross-section is evident, according with supposition presented in [21].

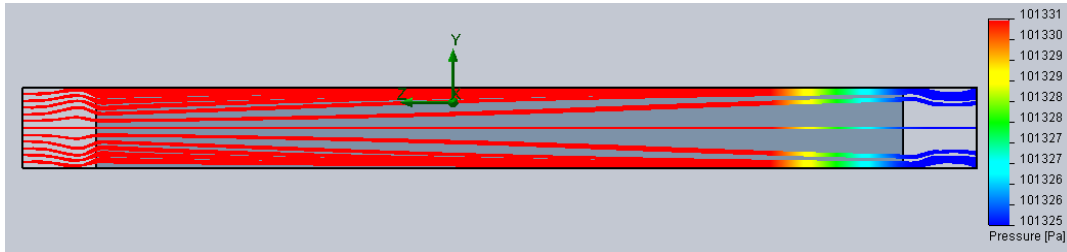


Figure 2: Side view of heat transfer medium pressure map in studied MF sample (porosity 85%). Medium flow (water): $Q = 2.08 \cdot 10^{-6} \text{ m}^3 \cdot \text{s}^{-1}$

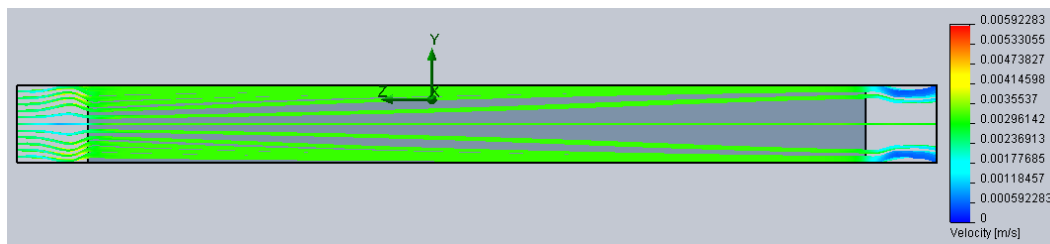


Figure 3: Side view of trajectories and heat transfer medium speeds in studied MF sample (porosity 85%), where homogenous laminar character of flow is evident. Medium flow (water): $Q = 2.08 \cdot 10^{-6} \text{ m}^3 \cdot \text{s}^{-1}$

Analysis results as a pressure loss in the graphical form are presented in Figure 4. Slightly exponential character of the behavior correlates with experiment results presented by Boomsma and his colleagues a Khayargoli1 and his colleagues in [21,16].

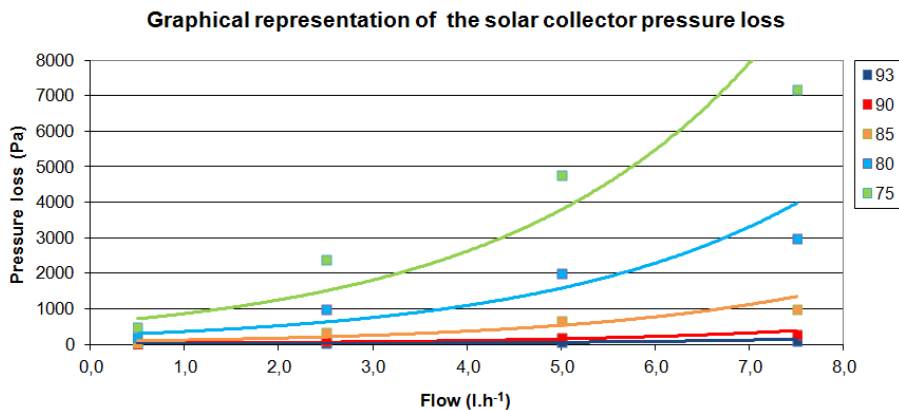


Figure 4: Solar collector absorber pressure loss behaviors.

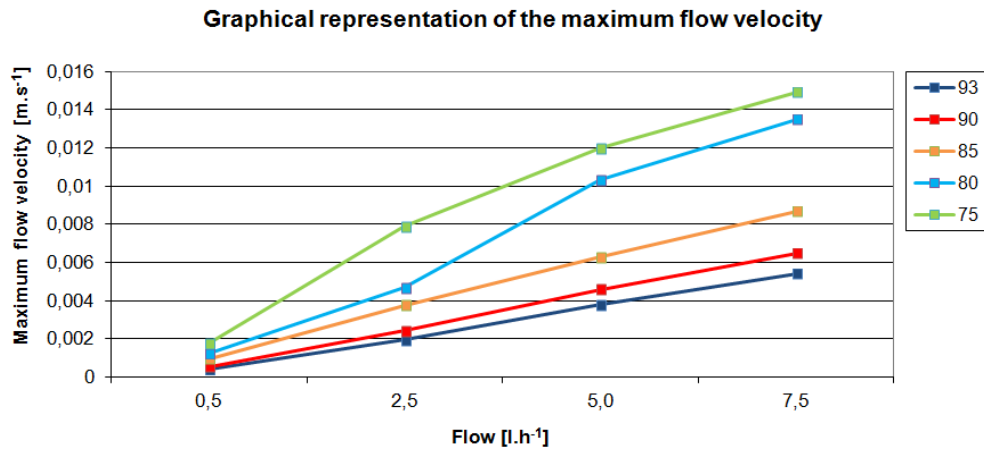


Figure 5: Maximal flow speeds in the solar collector absorber behaviors.

Heat transfer medium flow speed analysis (see Figure 5) results for maximal and average speeds show presence of areas with different maximal speeds behavior as was proposed in accordance with maximal speed curve line presented by Boomsma in [21]. This return us back to study of pressure maps and flow trajectories for each sample. The study subsequently showed that the behavior graphical forms differences are caused by flow turbulent character. This is a result of a acute pressure augmentation and a flow speed change when the heat transfer medium passing MF structure. This was also confirmed by Mostafid A., results published in [22], where he studied phenomena generated when heat transfer medium entry and appears MF. Graphical form of identified singularities are presented in Figure 6, where axial symmetry in y-z plane is evident.

The maximal flow speed characteristic shape shows until porosity 85% (45 PPI) linear flow character. Visible change of characteristic behavior is caused by flow transition from laminar to turbulent area. Heat transfer medium is intensively whirled in the absorber header channels, as a result of acute local hydraulic resistance augmentation and reduction. This is a reason of flow divergence in the flow profile periphery and formation of a area with quasi-null flow. Flow consolidation occurs after heat transfer medium outflow from MF structure during a medium flowing in the header output channel.

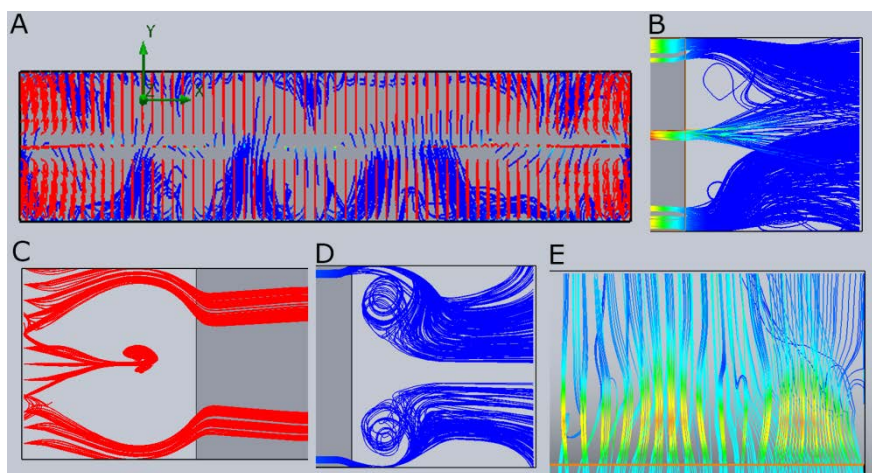


Figure 6: Singularities represented turbulent flow areas caused by heat transfer medium entering into MF

structure - view in y-x plane (a). The analogical effect on MF structure output – view y-z plane (b,c,d), view y axe (e). Header channels are colored in light gray. MF structure is colored in dark gray ($p=75\%$, flow $Q = 1.385 \cdot 10^{-7} \text{ m}^3 \cdot \text{s}^{-1}$).

A described phenomenon is a result of flow speed differences augmentation between space of input header, MF structure and output header, in the equation of continuity accordance. A flow speed augmentation behavior about $0.08 \text{ m} \cdot \text{s}^{-1}$ begins to demonstrate more significant level of pressure loss for MF $p=75\%$ (volume flow $2,5 \text{ l} \cdot \text{h}^{-1}$). Pressure loss augmentation from same level of volume flow is possible identified also for MF $p=80\%$.

5. Conclusion

In the paper presented results (pressure loss values, maximal and average speeds values, singularities formation conditions) shows the possibility to use MF structure for the intended purpose – lamella shape flow board creation as a full flow solar collector absorber. From hydraulic aspect is the more suitable MF with porosity 85 – 93% (45 – 15 PPI). A lower pressure loss reaches MF with higher porosity ($93\% = 15 \text{ PPI}$) and pressure loss of MF $p=85\%$ is only slightly higher. Average and maximal values of heat transfer medium flow speed in MF structure reaches minimal level for the same porosities. Significant declination of curve lines behavior was identified for MF with porosity 75% (159 PPI) and 80% (75PPI). Declinations are caused by singularities formation representing turbulent areas of flow in flow input and output from MF body. Pressure loss in MF body represents the most important parameter from the absorber design point of view, determined all another possible ways of hydraulic and heat-transfer design aspects. Due to the achieving similar results as other authors representing their experimentally gained results in similar conditions and in shape and dimensions similar objects it is possible to state relevancy of our results. Next movement of MF absorber development on gained results is possible to base. The first step is to build experimental lamella-shape MF absorber board in the full flow conception solar collector body. The relevance of full flow conception of riser channel was proven. We have got to state, that MF structures implementation into the solar thermal device is perspective respectively a combination of high value of specific heat transfer surface and full cross section flow type possibility.

References

- [1] M. Kaviany. Principles of heat transfer in porous media. New York, NY: Springer, 1995.
- [2] D.B. Ingham and I. Pop. Transport phenomena in porous media II. Oxford: Pergamon, 2005.
- [3] A. Bhattacharya, et al. "Thermophysical properties of high-porosity metal foams." *Int J of Heat and Mass Transfer*, vol. 45, pp. 1017-1031, 2002.
- [4] C.Y. Zhao. "Review on thermal transport in high porosity cellular metal foams with open cells.", *Int J of Heat and Mass Transfer*, vol. 55, pp. 3618 - 3632, 2012.
- [5] B. Ozmat, et. al. "Thermal applications of open cell metal foams." *Materials and Manufacturing Processes*, vol. 19, 839-862, 2004.
- [6] M. Hening. "Solar-thermal absorber, has metal foam thermally and conductively connected with cover on side turned toward incident sunlight after installation, where cover is coated with black color." Patent DE102009040039(A1). 28. 8. 2009.

- [7] L. Yongxin Zheng Fan. "Double-pipe high-efficiency foam metal heat exchanger." Patent CN201392115 (Y). 17. 03. 2009.
- [8] R. Rybár. "Inovative solutions in the field of solar heat technology as a development tool of renewable energy sources." Habilitation thesis. FBERG TU v Košiciach, Košice, 2006.
- [9] R. Rybár, P. Tauš and M. Cehlár. Solar energy and heliotechnics. Košice: FBERG TU, 2009.
- [10] R. Rybár, J. Horodníková and S. Perunko. "Development of non-metal medium temperature solar collector." *Energie* 21, vol. 4, pp. 34-35, 2011.
- [11] R. Rybár, J. Horodníková, D. Kudelas and M. Beer. "Considering the possibility of applying the structures based on metal foams in the construction of solar collector absorber." in Proc. ALER 2011: Alternative energy sources, 2011, pp. 18-25.
- [12] V. Adzhiev, E. Kartasheva and T. Kunii. "Cellular functional modeling of heterogeneous objects." in Proc. ACM Symposium on Solid Modeling and Applications, 2002.
- [13] C. Schroeder, W. Reglia, A. Shokoufandeh and W. Sun. "Computer-aided design of porous artifacts." *Computer-aided design*, vol. 37, 2005.
- [14] H. Darcy, H. Les fontaines publiques de la ville de Dijon. Dalmont, 1856.
- [15] E. Kruger. Die Grundwasserbewegung. Internationale Mitteilungen für Bodenkunde, 1918.
- [16] P. Khayargoli, V. Loya, L. Lefebvre, L., M. Medraj. "The impact of microstructure on the permeability of metal foams." Proc. CSME Forum, 2004.
- [17] P. A. Davis, et al., "Application of a validation strategy to Darcy's experiment.", *Advances in Water Resources*, vol. 15, pp. 175-180, 1992.
- [18] K. Boomsma and D. Poulikakos. "The effects of Compression and Pore Size Variations on the Liquid Flow Characteristics in Metal Foams." *J of Fluid Engineering*, vol. 124, pp. 263-272, 2002.
- [19] C. Beckermann and R. Viskanta. "Forced convection boundary layer flow and heat transfer along a flat plate embedded in a porous medium.", *Int J of Heat and Mass Transfer*, vol. 30, pp. 1547-1551, 1986.
- [20] Solidworks Flow Simulation 2009 .Technical References. SolidWorks CORP, 2009.
- [21] K. Boomsma, D. Poulikakos and F. Zwick. "Metal foams as compact high performance heat exchangers." *Mechanics of Materials*, vol. 35, pp. 1161-1176, 2003.
- [22] A. Mostafid. "Entrance and Exit Effects on Flow through Metallic Foams." Thesis. The department of Mechanical Engineering Concordia University, Montreal, 2007.